

Luminescence and IR Characterization of Acid Sites on Alumina

Yan-Fei Shen*, Steven L. Suib,^{*†,1} Michel Deeba,[‡] and Gerald S. Koermer[‡]

^{*}Department of Chemistry, University of Connecticut, Storrs, Connecticut 06269-3060; [†]Department of Chemical Engineering, University of Connecticut, Storrs, Connecticut 06269; and [‡]Engelhard Corporation, Menlo Park, CN 28 Edison, New Jersey 08818

Received November 17, 1992; revised September 20, 1993

Luminescence and infrared (IR) spectroscopies of pyridine and ammonia adsorption have been used to measure acidities of γ -alumina. Neither luminescence nor IR spectra of pyridine adsorption show any Brønsted acidity on γ -alumina pretreated at 400°C. However, luminescence emission data reveal four weak OH bands even when pretreatment is done at 600°C. Pyridine and subsequent water adsorption yield six luminescence emission bands. A red shift of the pyridine emission band is found when pretreatment or desorption temperature is increased. IR spectra of ammonia on alumina pretreated at 400°C show three deformation bands at 1452, 1465, and 1485 cm^{-1} . The first band is also observed together with a band at 1554 cm^{-1} even for pretreatment at 950°C, and it corresponds to NH_4^+ formed from dissociative adsorption of ammonia, while the other two bands are assigned to ammonia adsorbed on Brønsted acid sites. These two bands disappear along with the appearance of a new band at 1429 cm^{-1} , when deuterated alumina is pretreated at 400°C and subsequently subjected to ammonia. This new band at 1429 cm^{-1} is due to NH_3D^+ formed from ammonia adsorbed on acidic OD sites. Consequently, ammonia IR results demonstrate the existence of Brønsted acid sites on alumina pretreated at 400°C. © 1994 Academic Press, Inc.

INTRODUCTION

Acidity of γ -alumina has been extensively investigated. However, the existence of intrinsic Brønsted (B) acid sites is still controversial. Only Lewis (L) acidity was observed for spectroscopic studies of pyridine adsorption (1–4) and model catalytic reactions (5, 6). In contrast, weak B-acid sites were claimed from either spectroscopic studies (7–10) or model reactions (11, 12).

On the other hand, the nature of surface OH species on Al_2O_3 continues to generate considerable interest. Peri (13) and Knözinger and Ratnasamy (14) have proposed models to discriminate five OH IR bands (3). The existence of six different OH species has been assumed (15).

Many techniques have been developed for acidity measurements, such as TPD, IR, NMR, and XPS. Moreover,

luminescence was also used to probe Lewis acidities (16, 17) and surface hydroxyl groups (18–21) of some oxides and zeolites.

Luminescence excitation, emission, and lifetimes are sensitive experiments, due to the intrinsically high information content (selectivity). Considerable structural information can be obtained, such as the nature of adsorbed species and interfacial dynamics as well as the environment of fluorophores (22).

Luminescence methods have been successfully used to study (a) the environment of rare earth cations in zeolites (23), (b) poisoning mechanisms of fluid catalytic cracking (FCC) catalysts by vanadium and nickel (24), and (c) the determination of acid sites (17).

The present study attempts to further develop this technique for measurements of acidities. γ -alumina has been chosen as a support.

EXPERIMENTAL

1. Sample Preparation

γ -alumina was obtained from Engelhard Corporation in a powder form. Prior to being used, it was pressed into pellets, and subsequently ground and sieved. A fraction of particles with size of 20–50 mesh were chosen. After the particles were evacuated overnight at room temperature to pump out residual fine powder, they were loaded into an *in situ* quartz sample cell for thermal pretreatment and adsorption/desorption of pyridine.

Before pyridine adsorption, γ -alumina was pretreated at a desired temperature under a vacuum of about 5×10^{-5} Torr for 8 hr or more. After pretreatment, the sample was cooled to room temperature and a “blank” fluorescence spectrum was taken. Subsequently, pyridine was adsorbed at room temperature and then evacuated to a pressure less than 1×10^{-4} Torr at 100°C intervals from room temperature to 600°C. Adsorbed amounts were weighed (17) and luminescence measurements were performed after each step.

¹ To whom correspondence should be addressed.

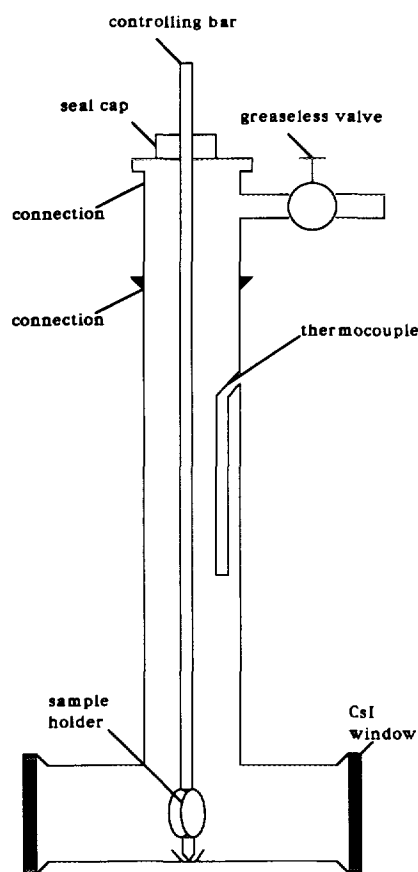


FIG. 1. Diagram of IR cell for pyridine and ammonia adsorption.

2. Luminescence Measurements

Fluorescence emission spectra were recorded at room temperature with a Spex Model 1680 202B double monochromator spectrometer. The front face mode was chosen, along with band pass slits of 1.0 nm. A Rhodamine B solution was used as a reference in order to correct for variations in intensity of the arc lamp excitation.

3. FTIR Measurements

IR spectra of adsorbed pyridine were recorded for comparison to luminescence results. An *in situ* IR cell was designed, as shown in Fig. 1. The sample holder was connected to a controlling rod, which could move under high vacuum conditions. A sample wafer was subjected to pretreatment and/or adsorption in the heating area. The temperature of this cell can be measured quite precisely since a thermocouple is mounted close to the sample wafer. After pretreatment, the wafer was moved down into the analysis chamber for IR measurements. CsI or NaCl single crystals are used as the cell windows. Pressure can be as low as 1×10^{-6} Torr in the evacuated cell.

A 10–20-mg self-supporting sample wafer was thermally pretreated at a certain temperature under vacuum (ca. 5×10^{-5} Torr) for 3 h. A Fourier transform infrared (FTIR) spectrum was recorded at room temperature with a Galaxy Model 4020 FTIR spectrometer. The wafer was exposed to pyridine vapor, which was purified with an activated 4A zeolite to remove water and also with the freeze–pump–thaw technique to eliminate trapped gas at room temperature for 30 min. Finally, desorption was carried out at different temperatures under a vacuum of ca. 10^{-5} Torr for 1 hr, before IR spectra of adsorbed pyridine were taken. For comparison with pyridine, ammonia (99.99%) that was further purified with BaO was used.

Since the present study emphasized the determination of acid sites, only IR spectral characteristics of acid sites will be reported; that is, only deformation modes will be presented.

RESULTS

1. Luminescence Measurements of OH Species and Acidities

Figure 2 presents emission spectra of pyridine adsorbed on γ -alumina pretreated at 400, 500, and 600°C and excited at 290 nm. At 400°C, a very broad spectrum, which consists of at least four peaks around 340, 377, 430, and 480 nm (Fig. 2a) is observed. The latter two peaks are stronger than the former two. If pretreatment is done at 500°C (Fig. 2b), there is a strong peak at about 330 nm, which is due to adsorbed pyridine, accompanied by a broad weak peak around 420–440 nm and almost no

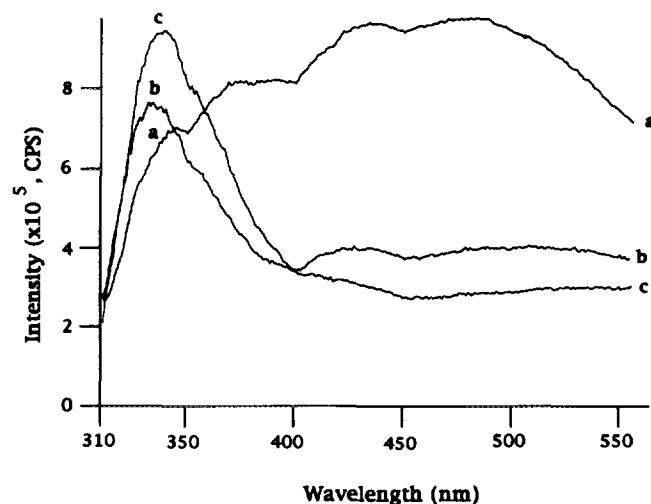
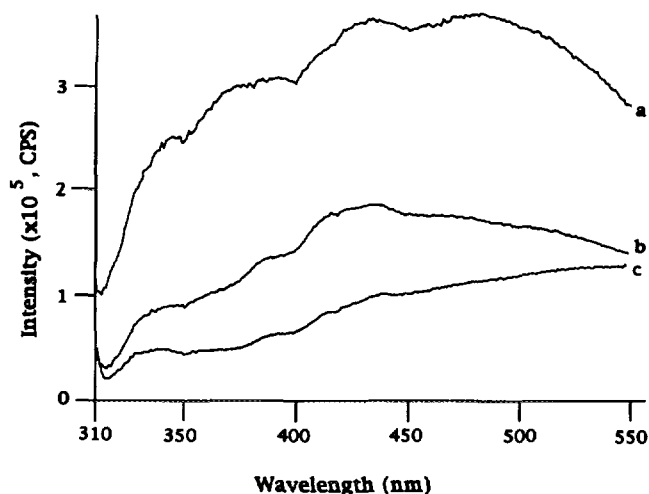


FIG. 2. Luminescence emission spectra of pyridine adsorbed on γ -alumina and desorbed at room temperature. The alumina was pretreated in vacuum at (a) 400°C, (b) 500°C, and (c) 600°C.

TABLE 1

Effects of Pretreatment Temperature on Luminescence Emission of OH Species and Adsorbed Pyridine on γ -Alumina

T_p ($^{\circ}\text{C}$)	OH bands (nm)	Pyridine band (nm)
400	340–346, 370–380, 425–445, 470–520	Not observed
500	425–440, 370–380, 340–350, >470	330
600	340–350, 370–380, 425–445, >470	340

FIG. 3. Luminescence emission spectra of γ -alumina pretreated in vacuum at (a) 400 $^{\circ}\text{C}$, (b) 500 $^{\circ}\text{C}$, and (c) 600 $^{\circ}\text{C}$.

peak near 480 nm. At 600 $^{\circ}\text{C}$, the adsorbed pyridine peak is intensified and shifted to about 340 nm, while the other peaks almost completely disappear (Fig. 2c).

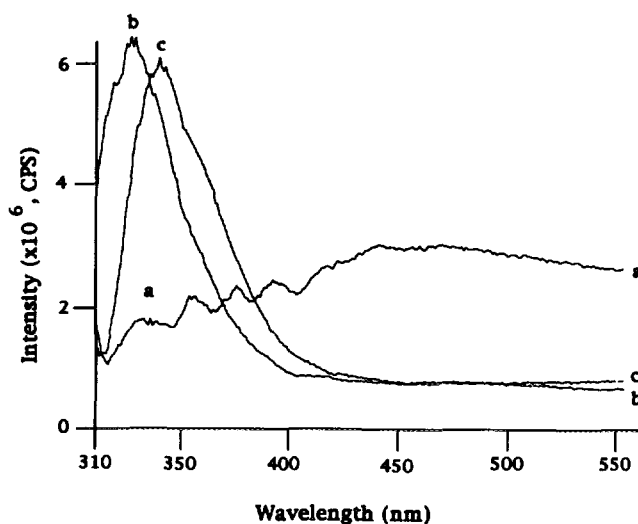
To assign the observed peaks, spectra of alumina dehydrated at 400, 500, and 600 $^{\circ}\text{C}$ are recorded, as shown in Fig. 3. At 400 $^{\circ}\text{C}$, at least four bands are observed around 340–346, 370–380, 425–445, and 470–520 nm (Fig. 3a). At 500 $^{\circ}\text{C}$, the band at 425–440 nm dominates, while the other bands largely decrease in intensity. At 600 $^{\circ}\text{C}$, all four bands are significantly decreased, though weak peaks are still observed at about 330–340, 380, 420, and 440 nm, together with a very broad band around 470–550 nm. These results, compared to those shown in Fig. 2, lead us to assign the peaks at 377, 430, and 480 nm in Fig. 2 to OH species rather than pyridine phosphorescence. Emission from OH species has been observed by others (18, 25) in this region for Al_2O_3 , which will be discussed below. In addition, the luminescence results, together with gravimetric data that suggest a considerable amount of pyridine adsorbed on alumina dehydrated at 400 $^{\circ}\text{C}$, indicate that surface OH species have a quenching effect on pyridine, but pyridine appears to have no such effect on OH species.

To clarify the interaction of adsorbed pyridine with OH species, the alumina, which is pretreated at 600 $^{\circ}\text{C}$ in vacuum and preadsorbed with pyridine vapor, is exposed to water vapor at room temperature and then desorbed at different temperatures. The spectra are shown in Fig. 4. When pretreatment is done at 100 $^{\circ}\text{C}$ (Fig. 4a), there are four clear emission peaks at 340, 356, 377, and 392 nm as well as a very broad band in the region of 410–550 nm which consists of at least two peaks. At 200 $^{\circ}\text{C}$, a strong peak at 325 nm is observed together with the other weak peaks (not shown here). At 400 $^{\circ}\text{C}$, only the pyridine peak

is detected at 330 nm (Fig. 4b). At 600 $^{\circ}\text{C}$, the pyridine peak is red shifted to 340 nm (Fig. 4c). These results suggest strong interactions between adsorbed pyridine and water on the surface of alumina. All luminescence data are summarized in Table 1.

2. IR Measurements of Pyridine Adsorption

Figure 5 shows the effect of pretreatment temperature on IR spectra of pyridine adsorption on γ -alumina. There is no band around 1540–1550 cm^{-1} , indicating there are no Brønsted acid sites on the three alumina samples. The intensity and shape of band at 1442 cm^{-1} relative to 1490 cm^{-1} are similar for the three samples, indicating there is no significant difference in the nature of NH_3 adsorbed on Lewis acid sites. The main difference is the relative intensity of the band at 1593 cm^{-1} with respect to the band at 1610 cm^{-1} . The bands at 1593 and 1610 cm^{-1} are assigned to hydrogen-bonded pyridine and coordinatively bonded pyridine, respectively. After pretreatment at 400 $^{\circ}\text{C}$, the H-bonded band is stronger than the coordinatively bonded band (Fig. 5a). At 500 $^{\circ}\text{C}$, the relative

FIG. 4. Luminescence emission spectra of water adsorbed on pyridine preadsorbed on γ -alumina and desorbed at (a) 100 $^{\circ}\text{C}$, (b) 400 $^{\circ}\text{C}$, and (c) 600 $^{\circ}\text{C}$.

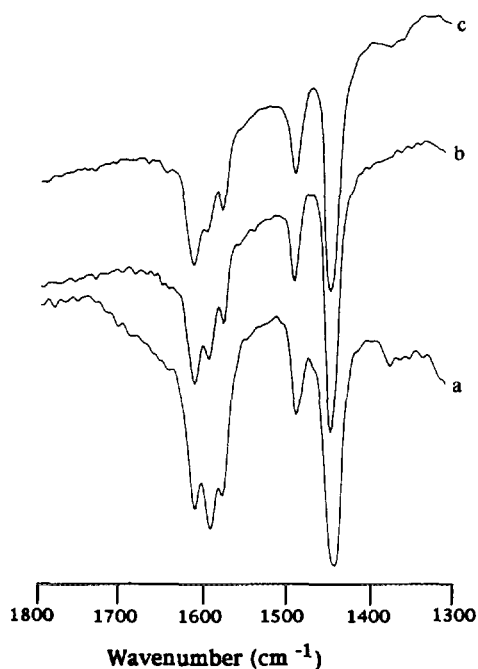


FIG. 5. IR spectra of pyridine adsorbed on γ -alumina pretreated in vacuum at (a) 400°C, (b) 500°C, and (c) 600°C. Desorption is done in vacuum at room temperature.

intensity of the H-bonded band to the coordinatively bonded band decreases (Fig. 5b). At 600°C, there is still an observable H-bonded band, indicating the existence of OH species on the alumina pretreated at 600°C, though the OH species is not acidic enough to form pyridinium cations. These results agree well with the above luminescence emission spectra, which indicate a decrease in OH species with increasing pretreatment temperature and the existence of OH species on the alumina heated at 600°C (Figs. 3 and 5).

3. IR Measurements of Ammonia Adsorption

Figure 6 shows IR spectra for ammonia adsorption at room temperature on alumina pretreated under vacuum at 400°C for 3 hr. When subsequent desorption is performed in vacuum at room temperature for 1 hr, two broad bands are observed around 1620 and 1450–1490 cm^{-1} (Fig. 6a). The former band has been assigned to NH_3 adsorbed on Lewis acid sites. The latter broad band consists of three peaks at 1452, 1465, and 1485 cm^{-1} that may be assigned to ammonia adsorbed on three different OH species, since the bands in this region are characteristic of NH_4^+ . When further evacuation is carried out at room temperature for longer time (20 hr), the intensity of the peak at 1452 cm^{-1} relative to that of the peaks at 1465 and 1485 cm^{-1} increases, and a shoulder appears at 1577 cm^{-1} . Desorption at 100°C for 1 hr further increases the

relative intensity of the peak at 1452 cm^{-1} and the peak at 1577 cm^{-1} (Fig. 6b). In addition, the two bands at 1465 and 1485 cm^{-1} are shifted to 1477 and 1491 cm^{-1} , respectively. With desorption temperature further increasing to 200 and 300°C (Figs. 6c and 6d), the intensity of the bands at 1452 and 1577 cm^{-1} relative to the bands at 1477, 1591, and 1616 cm^{-1} increases.

When pretreatment is performed at 600°C for 3 hr, followed by ammonia adsorption at 100 Torr and room temperature for 5 min and then by desorption at room temperature for a few hours, four bands at 1452, 1491, 1554, and 1620 cm^{-1} are observed (Fig. 7a). With desorption temperature increasing, the band at 1620 cm^{-1} is weakened, while the band at 1452 cm^{-1} is intensified (Figs. 7b–7d). The band at 1554 cm^{-1} , due to NH_2 species, disappears and a new peak at about 1580 cm^{-1} appears at 200°C. The band at 1452 cm^{-1} is still strong after desorption at 400°C (Fig. 7e).

When alumina is pretreated at 950°C, where no OH species are detected, and subject to ammonia adsorption at room temperature and 100 Torr, desorption at room temperature leads to four bands at 1452, 1515, 1554, and 1612 cm^{-1} (Fig. 8a). When desorption temperature is increased to 100°C, the bands at 1515 and 1554 cm^{-1} due to NH_2 species disappear, while the band at 1452 cm^{-1} is intensified. The band at 1612 cm^{-1} is shifted and splits into two peaks at about 1605 and 1580 cm^{-1} . Further increasing desorption temperature decreases the intensity of the bands at 1452, 1580, and 1605 cm^{-1} (Figs. 8c and 8d). After desorption at 500°C (Fig. 8e), these three

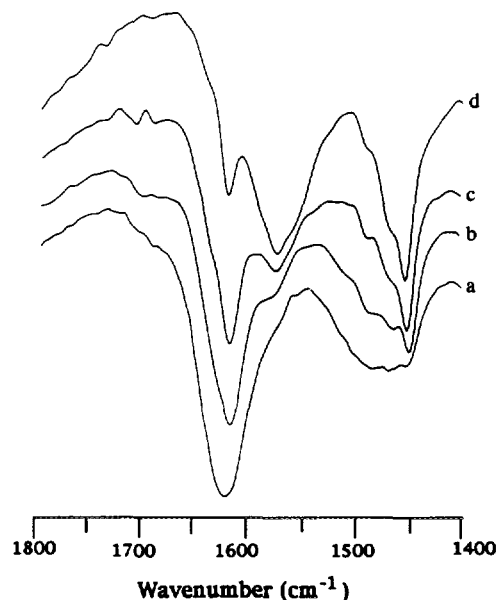


FIG. 6. IR spectra of ammonia adsorbed on γ -alumina pretreated in vacuum at 400°C and subsequently desorbed at (a) 25°C, (b) 100°C, (c) 200°C, and (d) 300°C.

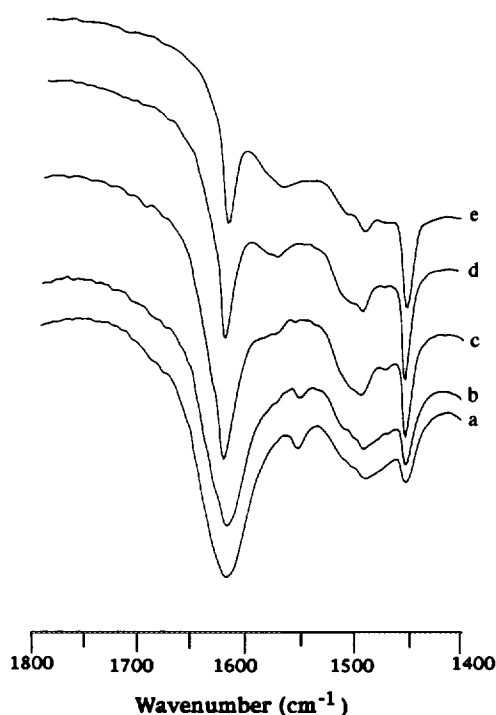


FIG. 7. IR spectra of ammonia adsorbed on γ -alumina pretreated in vacuum at 600°C and subsequently desorbed at (a) 25°C, (b) 100°C, (c) 200°C, (d) 300°C, and (e) 400°C.

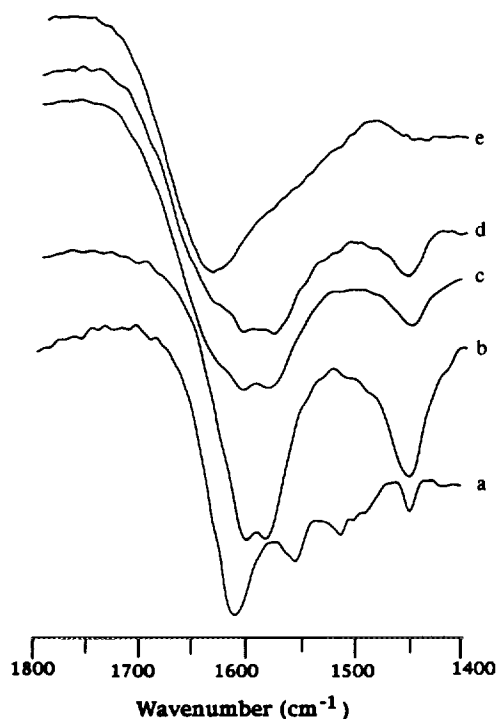


FIG. 8. IR spectra of ammonia adsorbed on γ -alumina pretreated in vacuum at 950°C and subsequently desorbed at (a) 25°C, (b) 100°C, (c) 200°C, (d) 300°C, and (e) 500°C.

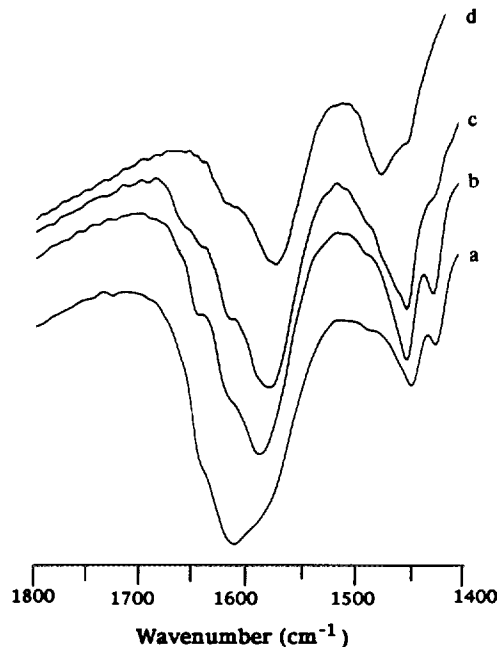


FIG. 9. IR spectra of ammonia adsorbed on deuterated γ -alumina pretreated in vacuum at 400°C and desorbed at (a) 25°C, (b) 100°C, (c) 200°C, and (d) 300°C.

bands at 1452, 1580, and 1605 cm^{-1} disappear and a broad peak at about 1645 cm^{-1} appears.

To further clarify ammonia adsorption on Brønsted acid sites, an alumina wafer is pretreated in vacuum at 600°C for 3 hr to remove most of the OH species, especially acidic OH species. The sample wafer is then exposed to D_2O vapor at room temperature for 10 min, followed by another pretreatment in vacuum at 400°C for 3 hr and ammonia adsorption at room temperature and 100 Torr for a few minutes. After desorption at various temperatures, spectra are taken, and they are shown in Fig. 9. At 25°C (Fig. 9a), a broad band centered at 1610 cm^{-1} , which appears to consist of three peaks at about 1590, 1610, and 1645 cm^{-1} , and two other bands at 1450 and 1429 cm^{-1} are detected. The band at 1450 cm^{-1} increases in intensity with increasing desorption temperature to 200°C (Figs. 9b and 9c). The band at 1429 cm^{-1} , which will be assigned to NDH_3^+ species, is still rather strong at 100°C (Fig. 9b) and almost disappears at 200°C (Fig. 9c). The bands at 1645 and 1610 cm^{-1} significantly decrease in intensity at 100°C, and the band at 1590 cm^{-1} becomes dominant (Fig. 9b). With temperature further increasing, the band at 1590 cm^{-1} is shifted toward lower wavenumbers (Fig. 9c and 9d). At 300°C, the band at 1429 cm^{-1} completely disappears, and a very weak peak at 1452 cm^{-1} and two peaks at 1489 and 1575 cm^{-1} appear (Fig. 9d).

In summary, the observed IR bands of adsorbed NH_3

TABLE 2
IR Data of Ammonia Adsorption on Alumina and Peak Assignments

Sample	T_p (°C)	Deformation band (cm^{-1})	Assignment
Al_2O_3	400	1620	Al-NH_3
		1452	NH_4^+
		1465	NH_4^+
		1485	NH_4^+
		1577	NH_2
	600	1452	NH_4^+
		1491	^a
		1554	Al-NH_2
		1515	Al-NH_2
		1580	NH_2
		1620	Al-NH_3
	950	1452	NH_4^+
		1554	Al-NH_2
		1515	Al-NH_2
		1512	Al-NH_3
1580		NH_2	
1602		Al-NH_3	
Deuterated Al_2O_3	400	1610	Al-NH_3
		1590	NH_2
		1645	^a
		1450	NH_4^+
		1429	DNH_3^+

^a Not assigned.

are listed in Table 2, along with band assignments, which will be discussed below.

DISCUSSION

1. Luminescence Studies

Aza-aromatics have been reported to show interesting luminescence spectra on interaction with acids. A red shift is found when it reacts with Lewis acids (26–30), while a blue shift is observed when it reacts with Brønsted acids (28–31). As shown in Figs. 2 and 4, such shifts are observed. When the pretreatment temperature increases from 500 to 600°C, the pyridine emission maximum is red shifted by 10 nm (Figs. 2b and 2c). Similarly, increasing desorption temperature from 400 to 600°C also induces a 10-nm red shift (Figs. 4b and 4c). Although it is hard to simultaneously distinguish pyridinium, H-bonded pyridine, and pyridine on Lewis acid sites, the red shift of the emission maximum appears to indicate an interaction between pyridine and OH or water. Such an interaction is also apparent from Figs. 2a and 4a, where pyridine emis-

sion bands at about 330–340 nm are strongly quenched, and where OH bands appear.

More information on OH species can be obtained from Figs. 3 and 4a. The four bands in Fig. 3 and six bands in Fig. 4a appear to correspond to different types of OH species. The assignment to OH species finds support from the literature. For example, Knözinger and his colleague, using an argon ion laser as an excitation source, observed a broad luminescence band, which is assigned to two types of OH species on alumina (25). On other oxides like MgO and ThO₂, emission is also observed for different surface OH groups resulting from charge transfer transitions of OH groups in low coordination (high index planes) (18). Our previous lifetime experiments show five OH species on alumina at 375, 410, 440, 470, and 520 nm (16).

Figure 3 indicates a band around 340–346 nm and bands in the region of 360–540 nm. The bands in the region of 360–540 nm have been determined to be due to five OH species (16), as mentioned above. Therefore, Fig. 3 as well as Fig. 4a appears to indicate the presence of six OH species on alumina. The six OH species may correspond to the six OH species predicted by Yoshida (15), who claimed six OH species on the flat surfaces of (001), (111), and (110) as well as on stepped surfaces.

Figure 3 also shows that not all OH bands equally decrease in intensity as pretreatment temperature increases. This supports the assignment of the bands to different OH species rather than emission from different vibrational states of one OH species. The different dependence of the bands on temperature (Fig. 3) also explains differences in acidity of these OH species, as described elsewhere (14, 18). Hydrogen atoms of acidic OH species and basic OH species are more readily removed than neutral OH species. The band around 425–440 cm^{-1} in Fig. 3 may be assigned to neutral OH species, while the others are either acidic or basic.

2. IR Studies of Pyridine Adsorption

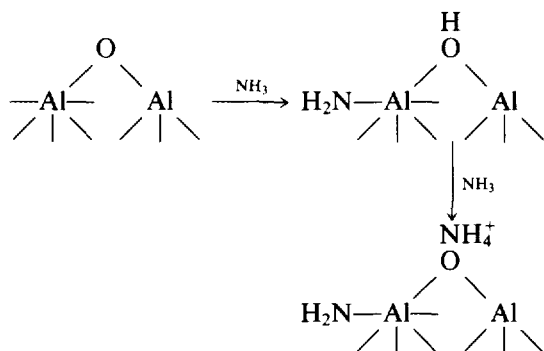
As in other reports (3, 13), no Brønsted acid sites are observed with pyridine adsorption. However, the H-bonding band at 1593 cm^{-1} (Fig. 5) shows the existence of OH species on the surface of the alumina pretreated even at 600°C. Though the type of the OH species cannot be assigned from the IR results, luminescence results in Fig. 3 show four weak OH emission bands. These four emission peaks, according to lifetime measurements (16), are due to four different OH species. As can be seen from Fig. 5, none of these four OH species is acidic enough to interact with pyridine to form pyridinium. However, one or more of these OH species can interact with stronger bases, such as 2,6-dialkyl substituted pyridine (8, 32, 33) and 2,6-lutidine (9), to form corresponding conjugated

acids. In other words, surface acidity is "relative," depending on the relative basicity of probe molecules.

3. Ammonia Adsorption Studies

Compared to pyridine ($K_b = 8.75$), ammonia is a stronger base ($K_b = 4.75$). Therefore, ammonia is expected to interact more strongly than pyridine with OH species to form corresponding conjugated acids. This is the general idea for the IR experiments with ammonia (Figs. 6–9) discussed below.

As shown in Fig. 6a, there are three bands at 1452, 1465, and 1485 cm^{-1} , probably corresponding to three types of NH_4^+ ions on γ -alumina pretreated at 400°C. With increasing desorption temperature, the band at 1425 cm^{-1} is intensified, while the other two bands are weakened. This difference may indicate the different nature of NH_4^+ species corresponding to the band at 1452 cm^{-1} and the other two bands. When pretreatment is complete at 600 or 950°C, where no acidic OH species exist, the band at 1452 cm^{-1} also appears (Figs. 7a and 8a), together with a band at 1554 cm^{-1} assigned to NH_2 species. These results indicate that the NH_4^+ species corresponding to the band at 1452 cm^{-1} may be formed through the process



where the bridging oxide ions are generally believed to be Lewis base sites (15, 34), while the corresponding OH species (bridged by an octahedral and a tetrahedral Al) are regarded as the most plausible Brønsted acid sites on dehydrated alumina (3, 15). Dissociative adsorption of ammonia on γ -alumina treated at elevated temperature has been well established. Although the peak at 1554 cm^{-1} is not clear in Fig. 6, the fact that its intensity increases with desorption temperature does not support the assignment of the peak to ammonia on Brønsted acid sites. Instead, this peak appears to be associated with a peak at about 1575–1590 cm^{-1} , which also increases in intensity with desorption temperature. According to a report (35), the peak at 1590 cm^{-1} is assumed to be another kind of surface NH_2 species. Primary amines and amides are also reported to have a band around 1600 cm^{-1} (13). The concurrent intensity change of the two bands at 1452 and ca. 1580 cm^{-1} with desorption tempera-

ture (Figs. 6–9) leads to the assignment of the band at ca. 1580 cm^{-1} to a kind of surface NH_2 species that may be more stable than other NH_2 species responsible for the band at 1554 cm^{-1} . These two kinds of NH_2 surface species may arise from NH_2 adsorbed on two different Al sites, though the nature of the sites is still unclear.

The bands at 1465 and 1485 cm^{-1} may be due to ammonia on Brønsted acid sites, i.e., due to NH_4^+ formed from the interaction between intrinsic surface OH species and ammonia. The decrease in the intensity of the band with desorption temperature supports this assignment. The disappearance of the band on deuterated alumina (Fig. 9) and the appearance of a new band at 1429 cm^{-1} also support the assignment. There are no literature data available for the band at 1429 cm^{-1} . However, it is reported (35, 36) that the ratios of the wavenumber of NH_2D , NHD_2 , and ND_3 to that of NH_3 are 0.92, 0.84, and 0.73–0.76, respectively. The corresponding values of NHD and ND_2 to that of NH_3 (34), and of ND_4^+ (1065 cm^{-1}) (37) to that of NH_4^+ (1450–1485 cm^{-1}) are 0.84, 0.74, and 0.72–0.73, respectively. These results indicate that the ratio only depends on the number of hydrogen atoms that are not replaced.

In order to explain the band at 1429 cm^{-1} , the following considerations have been made. Complete replacement of all hydrogen atoms by deuterium atoms gives a ratio of about 0.73, as can be seen in the cases of ND_4^+ , ND_3 , and ND_2 ; if one hydrogen atom is retained, the ratio is 0.84, as is the case for NHD and NHD_2 . Two hydrogen-containing species like NH_2D give a ratio of 0.92. Based on these assertions, therefore, the ratio of the wavenumber of NH_3D^+ to that of NH_4^+ should be higher than 0.92. A ratio of 0.97–0.98 is assumed to be reasonable here. This will give NH_3D^+ a bending band around 1421–1435 cm^{-1} , which agrees well with the band at 1429 cm^{-1} . Consequently, it is reasonable to assign the band at 1429 cm^{-1} to the NH_3D^+ species.

In conclusion, ammonia adsorption on γ -alumina and on its deuterated form reveals the existence of Brønsted acid sites on alumina pretreated at 400°C. NH_4^+ ions are also formed through dissociative adsorption of ammonia on the Al^+-O^- acid–base pair, especially at high temperatures.

When alumina is pretreated at a higher temperature, more basic oxide ions are created, multiple vacancy or defect sites are generated (3, 15), and aluminum cations are redispersed, favoring the occupation of tetrahedral sites (38). These results may help interpret the observed IR spectra of Figs. 7 and 8. The observation of the NH_4^+ band at 1452 cm^{-1} and the NH_2 bands at 1554 and 1510 cm^{-1} , which are not clearly observed when pretreatment is done at 400°C (Fig. 6), strongly demonstrates the creation of basic oxide ions and the dissociative adsorption of ammonia. As desorption temperature increases, the NH_2

band at 1554 cm^{-1} vanishes at 100°C (Fig. 8) or 200°C (Fig. 7), while another NH_2 band at $1580\text{--}1590\text{ cm}^{-1}$ gradually appears, as can be clearly seen from Fig. 8. Figure 6 also shows the appearance of a similar peak at about 1580 cm^{-1} at higher desorption temperature. This NH_2 peak should not be due to such a species as O-NH_2 , since an N-O stretching vibration at about 896 cm^{-1} is not found. Instead, this NH_2 species may be formed from disproportionation of ammonia probably adsorbed on octahedral aluminum ions, since the bands at about 1580 and 1452 cm^{-1} concurrently increase in intensity, together with a decrease in intensity of the band at 1610 cm^{-1} ascribed to NH_3 on Lewis acid sites (Fig. 8). In addition, increasing desorption temperature to 100°C shifts the peak maximum of the band at 1610 cm^{-1} to 1602 cm^{-1} . This may be due to adsorption of ammonia on different Lewis acid sites. As described above, multiple vacancy is created at a high temperature. This type of vacancy is expected to interact with ammonia more strongly than either $\text{Al}(\text{O}_\text{h})$ or $\text{Al}(\text{T}_\text{d})$ and may result in a lower N-H bending frequency.

CONCLUSIONS

Luminescence spectra show the presence of at least four OH bands on γ -alumina pretreated at 400°C and a red shift of the adsorbed pyridine band, as pretreatment or desorption temperature increases. There are strong interactions between OH surface species and adsorbed pyridine, which quench the emission of adsorbed pyridine species on alumina.

IR spectra of pyridine adsorbed on γ -alumina pretreated at 400°C or higher show no Brønsted acid sites. However, an H-bonded pyridine band is observed on alumina pretreated at temperatures as high as 600°C . Both luminescence and IR results show the existence of OH species on alumina surfaces pretreated at 600°C . IR spectra of ammonia adsorbed on alumina and on deuterated alumina pretreated at 400°C show the existence of Brønsted acid sites.

ACKNOWLEDGMENTS

We thank the Department of Energy, Office of Basic Energy Sciences, Division of Chemical Sciences, and Engelhard Corporation for support of this research.

REFERENCES

1. Parry, E. P., *J. Catal.* **2**, 371 (1963).
2. Medema, J., Van Bokhoven, J. J. G. M., and Kuiper, A. E. T., *J. Catal.* **25**, 238 (1972).
3. Knözinger, H., *Adv. Catal.* **25**, 184 (1976).
4. Ripmeester, J. A., *J. Am. Chem. Soc.* **105**, 2925 (1983).
5. Kania, W., *Bull. Acad. Pol. Sci., Ser. Sci. Chim.* **29**, 355, 365 (1982).
6. Gati, G., and Halasz, I., *J. Catal.* **82**, 223 (1983).
7. Kania, W., and Jurczyk, K., *Appl. Catal.* **61**, 27 (1990).
8. Dewing, J., Monks, G. T., and Youll, B., *J. Catal.* **44**, 226 (1976).
9. Corma, A., Rodellas, C., and Formes, V., *J. Catal.* **88**, 374 (1984).
10. Pearson, R. M., *J. Catal.* **46**, 279 (1977).
11. John, C. S., Tada, A., and Kennedy, L. V. F., *J. Chem. Soc., Faraday Trans. 1* **74**, 498 (1978).
12. Irvine, E. A., John, C. S., Kemball, C., Pearman, A. J., Day, M. A., and Sampson, R. J., *J. Catal.* **61**, 326 (1980).
13. Peri, J., *J. Phys. Chem.* **69**, 211, 220, 231 (1965).
14. Knözinger, H., and Ratnasamy, P., *Catal. Rev.* **17**, 31 (1978).
15. Yoshida, S., in "Theoretical Aspects of Heterogeneous Catalysis" (J. B. Moffat, Ed.), p. 506. Van Nostrand-Reinhold, Princeton, N.J., 1990.
16. Szedlacsek, P., Suib, S. L., Deeba, M., and Koermer, G. S., *J. Chem. Soc., Chem. Commun.* **21**, 1531 (1990).
17. Oelkrug, D. and Radjaipour, M., *Z. Phys. Chem.* **123**, 163 (1980).
18. Boehm, H. P., and Knözinger, H., in "Catalysis: Science and Technology" (J. R. Anderson and M. Boudart, Eds.), Vol. 4, p. 39. Springer-Verlag, New York/Berlin, 1983.
19. Steel, T. M., and Duley, W. W., *Astrophys. J.* **35**, 337 (1987).
20. Duley, W. W., *J. Chem. Soc., Faraday Trans. 1* **80**, 1173 (1984).
21. Coluccia, S., Deane, M., and Tench, A. J., in "Proceedings, 6th International Congress on Catalysis, London, 1976" (G. C. Bond, P. B. Wells, and F. C. Tompkins, Eds.), Vol. 1, p. 171. The Chemical Society, London, 1977.
22. Bright, F. V., *Spectroscopy (Eugene, Oreg.)* **5**(9), 33 (1990).
23. Tanguay, J. F., and Suib, S. L., *Catal. Rev.—Sci. Eng.* **29**(1), 1 (1987).
24. Anderson, M. W., Occelli, M. L., and Suib, S. L., *J. Catal.* **118**, 31 (1989).
25. Jeziorowski, H. and Knözinger, H., *Chem. Phys. Lett.* **51**, 519 (1977).
26. Weller, A., *Z. Elektrochem.* **61**, 956 (1957).
27. Kasama, K., Kikuchi, K., Yamamoto, S., Uji-ie, K., Nishida, Y., and Kokobum, K., *J. Phys. Chem.* **85**, 1291 (1981).
28. Uhl, S., and Oelkreg, D., *J. Mol. Struct.* **175**, 117 (1988).
29. Hensen, K., and Sarholz, W., *Theor. Chim. Acta* **12**, 206 (1968).
30. Karyakin, A. V., Sorokina, T. S., and Skvortsov, M. G., *Opt. Spectrosc. (Engl. Transl.)* **52**, 26 (1982).
31. Snyder, R., and Testa, A. C., *J. Phys. Chem.* **88**, 5948 (1984).
32. Knözinger, H., Krietenbrink, H., and Ratnasamay, P., *J. Catal.* **48**, 436 (1977).
33. Knözinger, H., and Stolz, H., *Ber. Bunsenges. Phys. Chem.* **75**, 1055 (1971).
34. Hindin, S. G., and Weller, S. W., *J. Phys. Chem.* **60**, 1501 (1956).
35. Tsyganenko, A. A., Pozdnyakov, D. V., and Filimonov, V. N., *J. Mol. Struct.* **29**, 299 (1975).
36. Morimoto, T., Yanai, H., and Nagao, M., *J. Phys. Chem.* **80**(5), 471 (1976).
37. Nakamoto, K., "Infrared and Raman Spectra of Inorganic and Coordination Compounds," 4th ed., p. 131. Wiley, New York, 1986.
38. Leonard, A. T., Semaille, P. N., and J. J. Fripiat, *Proc. Br. Ceram. Soc.*, 103 (1969).